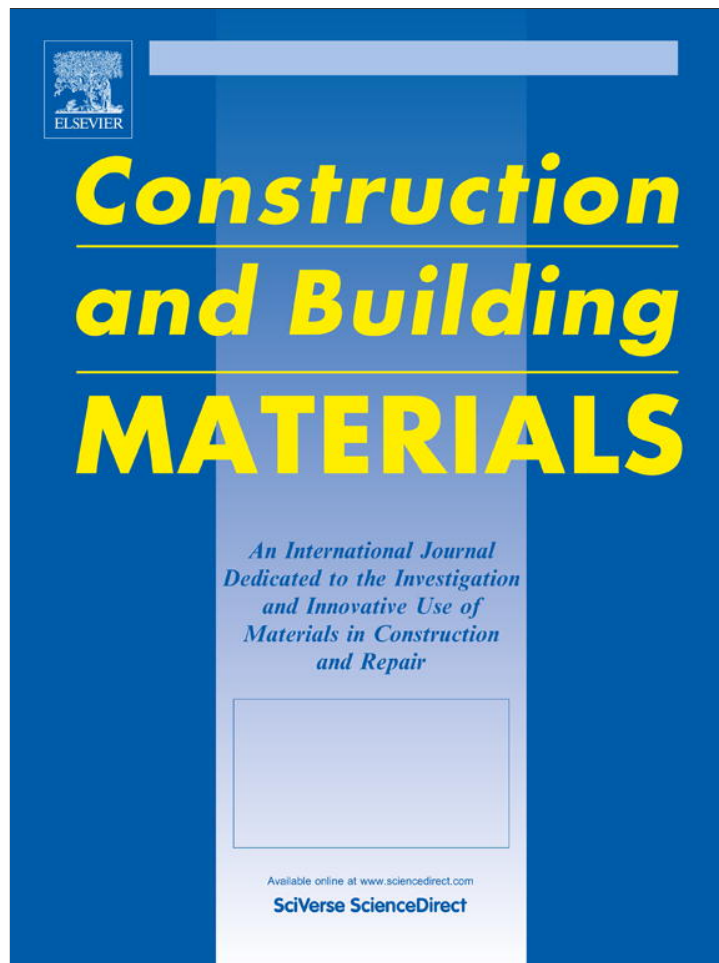


Provided for non-commercial research and education use.  
Not for reproduction, distribution or commercial use.



This article appeared in a journal published by Elsevier. The attached copy is furnished to the author for internal non-commercial research and education use, including for instruction at the authors institution and sharing with colleagues.

Other uses, including reproduction and distribution, or selling or licensing copies, or posting to personal, institutional or third party websites are prohibited.

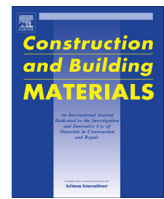
In most cases authors are permitted to post their version of the article (e.g. in Word or Tex form) to their personal website or institutional repository. Authors requiring further information regarding Elsevier's archiving and manuscript policies are encouraged to visit:

<http://www.elsevier.com/authorsrights>



Contents lists available at SciVerse ScienceDirect

# Construction and Building Materials

journal homepage: [www.elsevier.com/locate/conbuildmat](http://www.elsevier.com/locate/conbuildmat)

## Development of green engineered cementitious composites using iron ore tailings as aggregates

Xiaoyan Huang<sup>a</sup>, Ravi Ranade<sup>b</sup>, Wen Ni<sup>a</sup>, Victor C. Li<sup>c,b,\*</sup><sup>a</sup> State Key Laboratory of High-Efficient Mining and Safety of Metal Mines of Ministry of Education, University of Science and Technology Beijing, Beijing 100083, China<sup>b</sup> Department of Civil and Environmental Engineering, University of Michigan, Ann Arbor, MI 48109-2125, USA<sup>c</sup> Southeast University, Sipailou 2, Nanjing 210096, China

### H I G H L I G H T S

- Iron ore tailings (IOTs) were used as aggregates to prepare green ECC.
- Influences of IOTs size on fresh properties of ECC mortar were investigated.
- Influences of IOTs size on tensile properties of ECC were studied.
- The mechanical properties of ECC with IOTs are comparable to that with silica sand.

### A R T I C L E I N F O

#### Article history:

Received 22 January 2013

Received in revised form 15 March 2013

Accepted 22 March 2013

#### Keywords:

Engineered cementitious composites

Aggregate

Iron ore tailings

Fiber dispersion

Tensile ductility

### A B S T R A C T

Micro-silica sand is often used as fine aggregate in the production of Engineered Cementitious Composites (ECC), which is a class of ultra-ductile fiber-reinforced cement-based structural materials. However, high cost and limited availability of micro-silica sand creates an obstacle for widespread application of ECC in civil infrastructure. To overcome this limitation, the present study explores the feasibility of using iron ore tailings (IOTs) as cheaper and more environmentally friendly alternative aggregates without sacrificing the ductile mechanical performance of standard ECC. Influences of the size of IOTs on plastic viscosity of fresh ECC mortar, and on tensile properties and fiber dispersion in composites were experimentally investigated. At two levels of fly ash/cement ratio, performance of ECC with IOTs under direct tension and compression was investigated. The results show that ECC with IOTs as aggregates can attain tensile and compressive properties comparable to ECC with typically-used micro-silica sand, provided that the size of IOTs used is in the appropriate range which facilitates good fiber dispersion. Thus, the feasibility of using industrial solid waste-iron ore tailings as aggregates in the development of highly ductile and green ECC was established.

© 2013 Elsevier Ltd. All rights reserved.

## 1. Introduction

Engineered Cementitious Composites (ECC) designed through micromechanical principles are a special generation of high performance fiber reinforced cementitious composites, which are characterized by ultra-high tensile ductility and tight crack width [1]. ECC with 2% volume fraction of Poly-Vinyl Alcohol (PVA) fibers demonstrates a tensile strain capacity of 3–5%, which is two orders of magnitude higher than that of normal concrete and fiber reinforced concrete (FRC) [2]. Such high ductility is a result of tensile strain hardening behavior through multiple cracking. The inherently small crack width is typically below 100 μm even at large imposed tensile deformation [2]. Due to such high tensile ductility

and tight crack width, ECC exhibits superior durability compared to normal concrete and FRC under various mechanical and environmental conditions [3], making it a promising material to enhance safety, serviceability, and sustainability of civil infrastructure.

Aggregates in cementitious materials have a significant impact on material workability, strength, stiffness, shrinkage, and cost. Specifically, in ECC, aggregates influence the material's tensile performance mainly through alterations in matrix fracture toughness and fiber dispersion. The matrix fracture toughness tends to increase with larger aggregate size due to increase in tortuosity of fracture propagation. However, according to the micromechanical design principles of ECC, matrix fracture toughness has to be limited for attaining strain hardening behavior of the composite [1]. For this reason, coarse aggregate is not used in the standard ECC mixture [4]. Additionally, with the presence of PVA fibers in ECC, aggregates with size larger than average fiber spacing can

\* Corresponding author at: Department of Civil and Environmental Engineering, University of Michigan, Ann Arbor, MI 48109-2125, USA.

E-mail address: [vcli@umich.edu](mailto:vcli@umich.edu) (V.C. Li).

cause fiber clumping and poor fiber dispersion [5]. Fiber clumping becomes more pronounced with increase in aggregate size. Poor fiber dispersion leads to a reduction in the number of effective fibers at the failure crack, which causes a decrease in tensile strength and tensile strain capacity [6]. Therefore, in the design of ECC, the use of fine aggregate is needed to maintain low fracture toughness of the matrix and uniform fiber dispersion in the composite, both of which are crucial for achieving good tensile performance of ECC.

Due to the above considerations, micro-silica sand (SS) with an average diameter of approximately 110  $\mu\text{m}$  is frequently used in various ECC compositions [7–11]. However, the manufactured micro-silica sand is relatively expensive and is less widely available than common sand, which leads to higher initial cost of ECC. In addition, the initial energy consumption and CO<sub>2</sub> emissions associated with the manufacture of silica sand creates larger environmental burdens than coarser aggregates used in concrete. These initial economic and environmental costs limit large-scale application of ECC, despite the fact that replacement of a conventional material such as concrete with ECC in an infrastructure reduces the life cycle costs and environmental impact due to enhanced durability and less frequent maintenance [12]. Therefore, it is imperative to seek cost effective and environmentally friendly alternative aggregate in the production of ECC without sacrificing its mechanical properties.

This paper explores one of the several feasible approaches for promoting greenness and lowering cost of ECC by replacing micro-silica sand with iron ore tailings (IOTs). Iron ore tailings (IOTs) are waste ground rocks generated during the beneficiation process of iron ore concentration. In developing countries, IOTs are mainly stockpiled as waste and are often underutilized. For instance in China, the annual generation of IOTs increased from 137 billion ton in 2000 to 536 billion ton in 2009, and the total accumulation of IOTs from 2000 to 2009 exceeded 2.8 billion ton [13]. However, the current utilization rate of IOTs in China is less than 10% [14]. Due to the economic concern and environmental awareness, the reuse of IOTs is an urgent need. Utilization of IOTs in the production of ECC can potentially provide significant benefits in sustainability of both construction and mining industry, specifically, in terms of reductions in natural resource use, energy consumption, ECC cost, land use, and IOTs management cost.

This paper aims to investigate the feasibility of using IOTs as aggregates in the production of green ECC with reduced environmental and economic cost. The influences of the size of IOTs on plastic viscosity of fresh ECC mortar, fiber dispersion, and mechanical properties of ECC mixtures are experimentally investigated. The tensile and compressive properties of ECC with IOTs are compared to standard ECC with micro-silica sand at two different fly ash contents. Experimental investigations exploring various effects of IOTs on the mechanical performance of ECC and conclusions therefore are detailed in the following sections.

## 2. Experiment program

### 2.1. Materials

The major matrix ingredients of ECC are Type I ordinary Portland cement (C), Class F fly ash (FA), fine aggregate (IOTs or SS), water and High Range Water Reducing Admixture (HRWRA). Chemical composition and physical properties of fly ash are given in Table 1. Poly-Vinyl Alcohol (PVA) fibers are incorporated as reinforcing fibers. The PVA fibers with a length of 12 mm and diameter of 39  $\mu\text{m}$  are coated with 1.2% by weight of oil to control the fiber/matrix interfacial properties. The nominal tensile strength, elastic modulus, and density of the PVA fibers are 1620 MPa, 42.8 GPa, and 1300 kg/m<sup>3</sup>, respectively.

IOTs used in this study mainly consist of silica, alumina, and iron oxide, with quartz as the major mineral phase [15]. Four size ranges of IOTs depicted as IOTs-Fine, IOTs-1180, IOTs-600, and IOTs-425 were investigated in this study. During iron ore mining operations, two types of IOTs are generated, fine IOTs and

**Table 1**

Chemical and physical properties of fly ash (%).

Chemical composition, %	Fly ash
CaO	14.04
SiO <sub>2</sub>	44.09
Al <sub>2</sub> O <sub>3</sub>	23.21
Fe <sub>2</sub> O <sub>3</sub>	8.39
SO <sub>3</sub>	1.46
Moisture	0.05
Loss on ignition	0.56
Available alkalis, as Na <sub>2</sub> O	0.99
<i>Physical properties</i>	
Retained on 45 $\mu\text{m}$ , %	16.85
Water requirement, %	97
Specific gravity	2.45

coarse IOTs. The fine iron ore tailings as obtained from the mine without additional processing are named IOTs-Fine in this study. The coarse IOTs are passed through sieves with openings of 1180  $\mu\text{m}$ , 600  $\mu\text{m}$ , and 425  $\mu\text{m}$  (plus bottom pan) and the IOTs passing through sieve are called IOTs-1180, IOTs-600, and IOTs-425, respectively, such that the number in the name of IOTs represents the nominal maximum aggregate size. For comparison purpose, a standard ECC mixture containing micro-silica sand was also prepared. Particle size distributions of IOTs and micro-silica sand obtained through sieve analysis are given in Fig. 1. Particle morphology of micro-silica sand and IOTs-Fine is shown in Fig. 2, which suggests that micro-silica sand has a near-round shape, while IOTs have an angular shape as a result of crushing and grinding.

Alkali silica reaction (ASR) is known to cause serious deterioration problems in cementitious materials using aggregates containing amorphous silica, and therefore, the ASR potential of IOTs was determined before using it as alternative aggregate in ECC. Accelerated mortar bar test as specified by ASTM C 1260 was used to measure the ASR potential of IOTs. The mortar bars were immersed in a 1 N NaOH solution at 80 °C for 14 days. Fig. 3 shows the expansion test results of mortar bar specimens containing IOTs-Fine and IOTs-1180 as representatives of fine and coarse tailings, respectively. The expansion rate of these mortar bars measured at 14 days is far below 0.10% (Fig. 3), indicating that IOTs are innocuous aggregates that can be used in cementitious materials without concerns of ASR.

### 2.2. Mix proportions

Two sets of mixtures were prepared in this study. In the first set (Table 2), four ECC matrix mixtures M1–4 (without fibers, 'M' stands for matrix) with the same constituent proportions but with different IOTs size were prepared to investigate the influence of IOTs size on the plastic viscosity of fresh ECC mortar. The plastic viscosity was measured through Marsh cone flow test. The rheology of the matrix in the fresh state is important for fiber dispersion uniformity [6].

In the second set (Table 2) of mixtures, eight ECC mixtures C1–8 (with fibers, 'C' stands for composites) were prepared to investigate the effects of IOTs size and FA content (FA/C of 2.2 and 4.4 by mass) on the mechanical properties of cured ECC mixtures, while utilizing the knowledge of the influence of IOTs size on the fresh matrix properties from the first set to achieve good fiber dispersion in the second set. For mixtures C1–8, the HRWRA content was adjusted to keep the fresh matrix

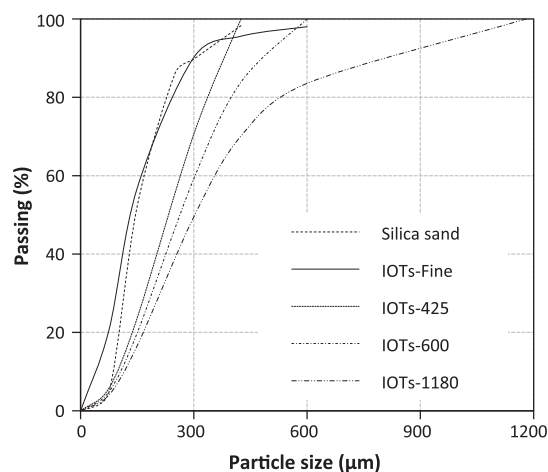


**Fig. 1.** Particle size distributions of IOTs and micro-silica sand.

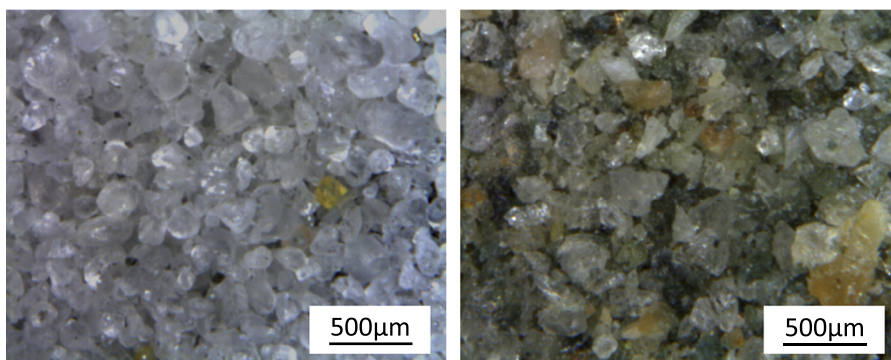


Fig. 2. Particle morphology of micro-silica sand and IOTs-Fine.

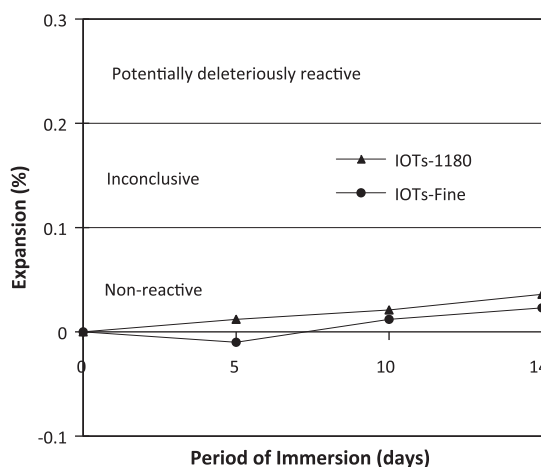


Fig. 3. Expansion of mortar bars as a function of immersion period.

viscosity of all mixtures at a constant level by maintaining the Marsh cone flow time of  $30 \pm 5$  s which was identified as the optimal range for achieving high degree of homogeneity of PVA fiber dispersion in ECC [6]. PVA fibers were used in all composite mixtures at a volume fraction of 2%. The mechanical properties of ECC with IOTs were also compared with standard ECC containing micro-silica sand (mixtures C7–8).

### 2.3. Specimens preparation

The matrices of all mixtures were prepared following a typical ECC matrix mixing procedure [15]. Marsh cone flow time of the fresh matrices of mixtures M1–4 was measured. For composite mixtures C1–8, desired Marsh cone flow time ( $30 \pm 5$  s, as mentioned above) of the fresh matrix mixtures was attained by adjusting the dosage of HRWRA. Subsequently, fibers were added and mixed with the matrices of C1–8. These freshly prepared mixtures were cast into molds that were

moderately vibrated using a vibration table. All specimens were demolded 1 day after casting and cured in a plastic bag at a room temperature of about  $23 \pm 3$  °C for another 27 days, when they were tested.

Three cube specimens measuring  $50 \times 50 \times 50$  mm<sup>3</sup> and three dogbone specimens were prepared for all composite mixtures C1–8 for compression and tension tests, respectively. The geometry of a dogbone specimen used in this study is given in Ranade et al. [16]. In addition, four notched beam specimens measuring  $305 \times 76 \times 38$  mm<sup>3</sup> for mixtures C1–4 were cast without adding fiber to determine the effect of IOTs size on the matrix fracture toughness.

### 2.4. Procedures of experiments

Marsh cone flow time was used to indirectly measure the plastic viscosity of fresh ECC mortar. The geometry of a Marsh cone is given in Li and Li [6]. It measures the time taken by a cone full of mortar to flow through a narrow opening at the bottom of the cone.

Uniaxial tension and compression tests were performed to characterize the tensile and compressive behavior of ECC mixtures C1–8. The direct tension tests on dogbone specimens were conducted at a controlled displacement rate of 0.5 mm/min as recommended by the Japan Society of Civil Engineers (JSCE) for direct tension testing of High Performance Fiber Reinforced Cementitious Composite [18]. Two LVDTs were attached on each dogbone specimen with gauge length of approximately 100 mm to measure the tensile extension. Compression tests were conducted in accordance with ASTM C109, and the peak compressive load was recorded to determine compressive strengths of various ECC mixtures.

The matrix fracture toughness was measured in accordance with ASTM E399 [17] using a three-point bending test setup. The span length of bottom support for the beam was 254 mm and the notch depth (at the longitudinal center of the beam) to beam height ratio was 0.4.

To investigate the influence of IOTs size on fiber dispersion, the degree of homogeneity of fiber dispersion in ECC mixtures C1–4 was determined using fluorescence microscopy and digital image analysis. After the uniaxial tension tests, a 5 mm-thick cross-section close to the final failure crack was cut perpendicular to the loading direction from each dogbone specimen (Fig. 4). In preparation for fluorescence imaging, these cross-sections were ground with p800 and p1200 sand papers for two minutes each. Subsequently, each cross-section was imaged at  $3.2\times$  magnification using a fluorescence microscope with a ultra-violet (UV) light source. The PVA fibers fluoresce and emit green light when excited by UV incident light while the surrounding cementitious matrix does not fluoresce and appears black, which differentiates fibers from matrix (Fig. 5). The field of view of the microscope is about

Table 2  
Mixture proportions.

Mix ID	Aggregate	C	FA/C	Aggregate/(FA + C)	Water/(FA + C)	HRWRA/(FA + C) (%)	PVA (vol.%)
M1	IOTs-Fine	1	2.2	0.36	0.26	0.40	–
M2	IOTs-425	1	2.2	0.36	0.26	0.40	–
M3	IOTs-600	1	2.2	0.36	0.26	0.40	–
M4	IOTs-1180	1	2.2	0.36	0.26	0.40	–
C1	IOTs-Fine	1	2.2	0.36	0.26	0.46	2.0
C2	IOTs -425	1	2.2	0.36	0.26	0.42	2.0
C3	IOTs-600	1	2.2	0.36	0.26	0.40	2.0
C4	IOTs-1180	1	2.2	0.36	0.26	0.37	2.0
C5	IOTs-Fine	1	4.4	0.36	0.26	0.42	2.0
C6	IOTs-425	1	4.4	0.36	0.26	0.40	2.0
C7	SS	1	4.4	0.36	0.26	0.42	2.0
C8	SS	1	2.2	0.36	0.26	0.43	2.0

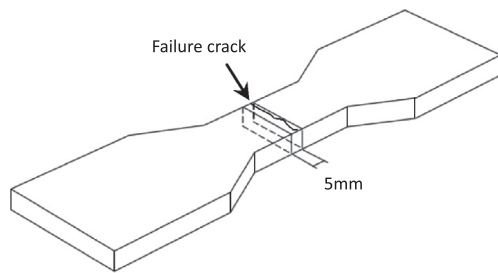


Fig. 4. Sample preparation for measuring fiber dispersion.

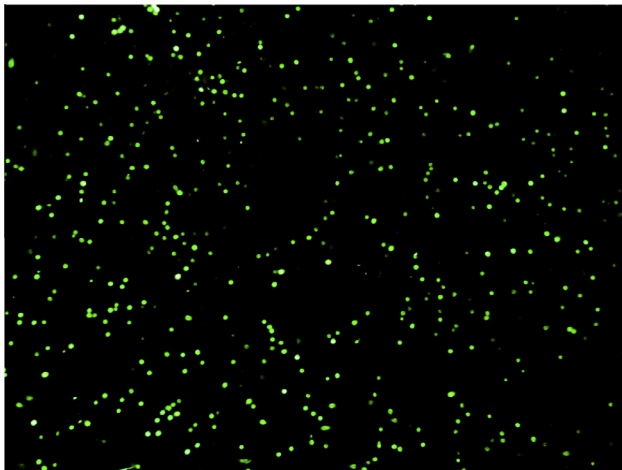


Fig. 5. Image captured on the cross-section under a fluorescence microscope.

$6.6 \times 5.0 \text{ mm}^2$ . A whole cross-sectional area cut from the dogbone specimens is  $30 \times 12.7 \text{ mm}^2$  and therefore eight images were taken for each section. A digital image processing method developed by Lee et al. [19] was used to calculate the fiber dispersion coefficient  $\alpha$  at these cross sectional images. The fiber dispersion coefficient  $\alpha$  was calculated according to the Eq. (1)

$$\alpha = \exp \left[ -\sqrt{\frac{\sum_{i=1}^n (x_i - 1)^2}{n}} \right] \quad (1)$$

where  $n$  is the total number of fibers detected in an image and  $x_i$  is the number of fibers observed in  $i$ th square. The entire image is considered to be divided in  $n$  equal squares.  $\alpha$  is 1, when there is exactly 1 fiber in each square (perfectly homogenous dispersion), whereas  $\alpha$  is almost equal to 0, when all fibers are clumped together in one square (no dispersion at all) [19].

### 3. Results and discussion

#### 3.1. Influence of IOTs size on the plastic viscosity of ECC matrix

Plastic viscosity of ECC matrix (before adding fibers) has significant impact on fiber dispersion and corresponding tensile ductility [6], and therefore, it is necessary to evaluate the influence of a new ingredient such as IOTs on the plastic viscosity. Marsh cone flow time was found to correlate well with the plastic viscosity of cementitious materials [6]. A longer marsh cone flow time indicates a higher plastic viscosity. It was concluded in a previous study [6] that the plastic viscosity corresponding to Marsh cone flow time of  $30 \pm 5 \text{ s}$  is desirable for achieving homogenous dispersion of PVA fibers in ECC matrix. The test results of the plastic viscosity of ECC matrix mixtures (M1–4) with the same mix proportions by weight but containing IOTs of differing sizes are summarized in Table 3. Among the mixtures M1–4, the Marsh cone flow time of only one mixture (M3) with IOTs-600 lies in the desirable range  $30 \pm 5 \text{ s}$ . Overall, it is observed that an increase in IOTs

Table 3

Influence of IOTs size on plastic viscosity of ECC matrix.

Mix ID	Aggregate	Marsh cone flow time (s)
M1	IOTs-Fine	Flow stopped (very long time)
M2	IOTs-425	60
M3	IOTs-600	28
M4	IOTs-1180	16

size (from M1 to M4) results in a decrease of the Marsh cone flow time of ECC matrix. This observation of decrease in matrix viscosity with increase in IOTs size is used to guide the design of matrices for the ECC (with fiber) mixtures discussed in the next section.

#### 3.2. Influence of IOTs size on the composite tensile behavior

As discussed above, the size of IOTs can potentially affect the fiber dispersion and, therefore, the mechanical properties of ECC in two ways. First, the IOTs size may influence the matrix viscosity (as noted in the previous section) which affects fiber dispersion, and second, the IOTs size may directly affect the available space between fibers for dispersion. In order to eliminate the effect of IOTs size on the viscosity of fresh ECC matrix (first way), the mass ratio of HRWRA to total cementitious materials (HRWRA/FA + C) in mixture C1–4 was varied from 0.37% to 0.46% (Table 3) for maintaining the Marsh cone flow time of  $30 \pm 5 \text{ s}$  in all composite mixtures. Using mixture M3 as the baseline, the HRWRA content is left unchanged (HRWRA/FA + C = 0.40% by weight) in the corresponding ECC mixture C3 (with fibers) containing IOTs-600, whereas it is increased for ECC mixtures with finer IOTs (C1–2) and decreased in ECC C4 containing coarser IOTs for obtaining target viscosity. Maintaining constant matrix viscosity ensures that the fiber dispersion and corresponding mechanical performance of the composite is not affected by the matrix viscosity and is mainly influenced by IOTs size effect on fiber spacing, which is the objective of investigation in this part of the study.

The uniaxial tensile test results of mixtures C1–4 at the age of 28 days are given in Fig. 6 and Table 4. Three dogbone specimens were tested for each mixture. It is observed that all ECC mixtures show strain hardening behavior with tensile strain capacities ranging from 1.5% to 2.9% at 28 days. The tensile strain capacities of ECC mixtures C1–4, normalized by the tensile strain capacity of mixture C1, are plotted against IOTs size in Fig. 7. It is observed that the tensile strain capacity of ECC mixtures decreases as the IOTs size increases. The reduction in tensile ductility is only marginal as the IOTs size increases from IOTs-Fine to IOTs-425, while the tensile ductility decreases substantially with further increase in IOTs size from IOTs-425 to IOTs-1180. Compared with mixture C1 containing IOTs-Fine, mixture C4 with IOTs-1180 exhibits nearly 50% reduction in tensile strain capacity. Therefore, IOTs-Fine and IOTs-425 are preferred as alternative aggregates in ECC in view of tensile ductility optimization.

In order to determine the underlying cause for the reduction in tensile ductility with larger IOTs, the effect of IOTs size on the fiber dispersion was investigated. As explained above (Eq. (1)), fiber dispersion can be quantified by fiber dispersion coefficient ( $\alpha$ ), which is computed from fluorescence images of material cross-sections. Higher fiber dispersion coefficient indicates more homogenous fiber dispersion. Fig. 8 shows the influence of IOTs size on the fiber dispersion coefficient. It is observed that an increase in IOTs size causes a reduction in fiber dispersion coefficient. The correlation between the fiber dispersion coefficient and the tensile strain capacity is plotted in Fig. 9. It is observed that there is a strong positive correlation between tensile strain capacity and fiber

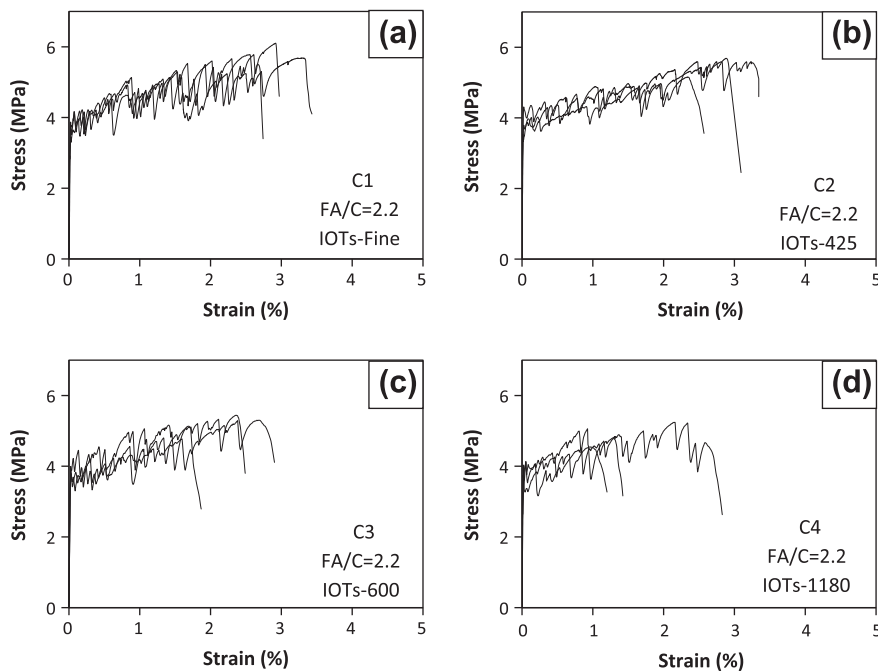


Fig. 6. Uniaxial tensile stress–strain curves for mixtures C1–4 at 28 days.

Table 4

Tensile properties of mixtures C1–4 at 28 days.

Mix ID	Aggregate size	First cracking strength (MPa)	Tensile strength (MPa)	Tensile strain (%)
C1	IOTs-Fine	3.8 ± 0.5	5.8 ± 0.3	2.9 ± 0.4
C2	IOTs-425	3.9 ± 0.4	5.6 ± 0.3	2.8 ± 0.6
C3	IOTs-600	3.9 ± 0.1	5.3 ± 0.4	2.4 ± 0.5
C4	IOTs-1180	4.0 ± 0.2	4.9 ± 0.6	1.5 ± 0.6

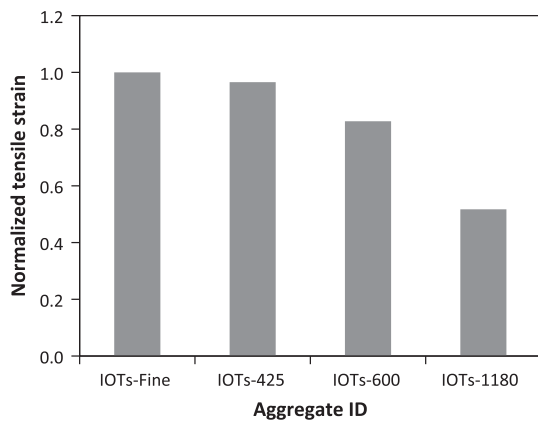


Fig. 7. Normalized tensile strain capacity of ECC mixtures with IOTs in various sizes.

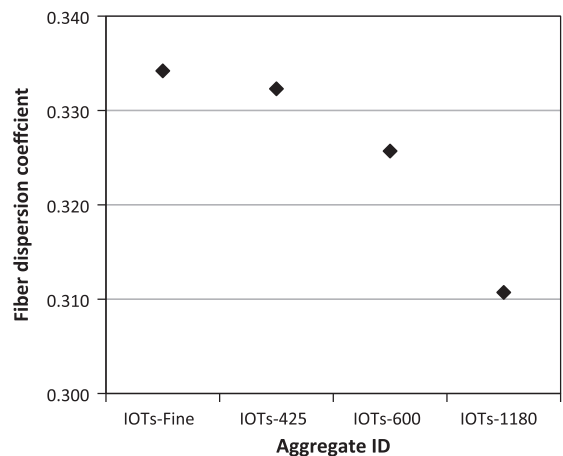


Fig. 8. Influence of IOTs size on fiber dispersion coefficient.

dispersion coefficient of ECC mixtures. These results suggest that ECC mixtures with coarser IOTs have lower fiber dispersion coefficient, which causes the observed reduction in tensile strain capacity of ECC.

The decrease in fiber dispersion coefficient with relatively coarser IOTs aggregate is likely due to the detrimental influence of large aggregate size on fiber dispersion, which is schematically illustrated in Fig. 10 [5]. Fiber clumps were felt by hand in the fresh mixture of C4 containing IOTs-1180 even though the matrix viscosity was controlled in the optimized range. Good fiber dispersion re-

quires aggregates to be small enough to move freely between the fibers [5]. Aggregates with particle size larger than the average distance between fibers may cause fiber clumping, as illustrated in Fig. 10; a theoretical discussion of this effect is presented in the following paragraph.

The theoretical distance ( $D$ ) between fibers, assuming that fibers are uniformly distributed (fiber dispersion coefficient,  $\alpha = 1$ ), can be calculated by Eq. (2). The theoretical number of fibers per unit area ( $N_B$ ) of the composite can be calculated using Eq. (3) [21].

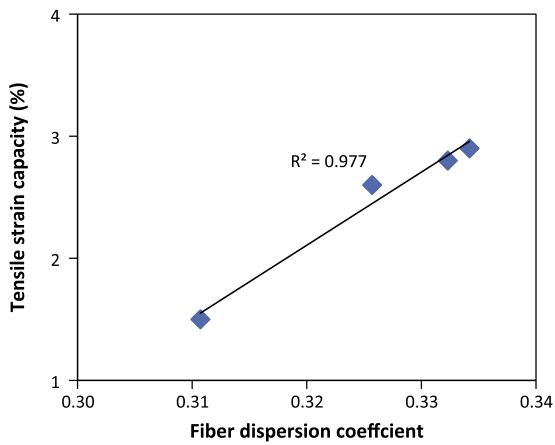


Fig. 9. Correlation between the fiber dispersion coefficient and the tensile strain capacity.

$$D = \sqrt{1/N_B} - d_f \quad (2)$$

$$N_B = \frac{V_f}{A_f} \eta_B \quad (3)$$

where  $d_f$  and  $A_f$  are fiber diameter and cross-sectional area, and  $V_f$  is the volume fraction of the fibers in the composite.  $\eta_B$  is the fiber bridging efficiency dependent on fiber orientation distribution; theoretical values of  $\eta_B$  are 1,  $2/\pi$ , and 0.5 for uniformly random 1D, 2D, and 3D fiber distributions, respectively.

For ECC mixtures containing PVA fibers with diameter ( $d_f$ ) of 39  $\mu\text{m}$  at volume fraction ( $V_f$ ) of 2% in this study, the theoretical number of fibers per square centimeter ( $N_B \times 1 \text{ cm}^2$ ) and fiber distance ( $D$ ) for three types of fiber orientation distributions are summarized in Table 5. The theoretical distance between fibers for 1D, 2D, and 3D distributions are 205  $\mu\text{m}$ , 267  $\mu\text{m}$ , and 307  $\mu\text{m}$ , respectively. In actual laboratory specimen or structural members, fiber orientation tends to be 2D or 3D distribution for short PVA fibers depending on the specimen/member geometry. Due to the inevitable non-homogeneity of fiber dispersion (signified by observed  $\alpha$  considerably less than 1) in real mix processing, the actual distance between the fibers might be greater than the theoretical values of 267  $\mu\text{m}$  or 307  $\mu\text{m}$  (for 2D and 3D distributions), and therefore, aggregates with maximum size considerably larger than these sizes are also acceptable to some extent. Nevertheless, the theoretical fiber distance serve as guidelines for choosing aggregates in an appropriate size range in combination with experimental observations. The experimental results of this study suggest that the aggregate size of IOTs-425 is the particle size limit for achieving optimal fiber dispersion coefficient in ECC mixtures as a more significant drop in fiber dispersion coefficient and mechanical performance of ECC mixtures is observed with IOTs coarser than IOTs-425.

Table 5  
Number of fibers per  $\text{cm}^2$  and distance between fibers for ECC with uniform fiber dispersion.

Fiber orientation	Number of fibers per $\text{cm}^2$	$D$ ( $\mu\text{m}$ )
1D	1675	205
2D (random)	1066	267
3D (random)	838	307

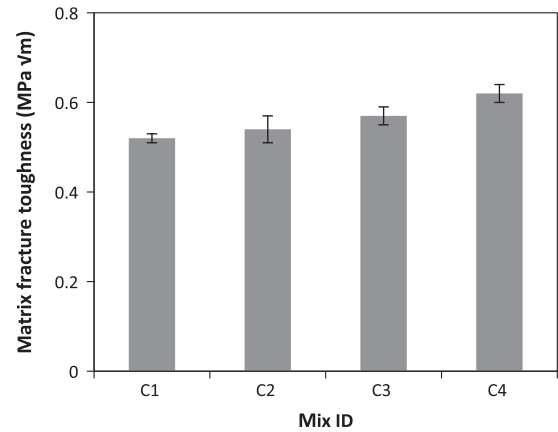


Fig. 11. Fracture toughness of matrices of mixtures C1–4 at 28 days.

The strain capacity reduction of ECC mixtures can also be partly explained by the increase of matrix fracture toughness. Fig. 11 shows the fracture toughness test results of the matrices (without adding fibers) of mixtures C1–4. As shown in Fig. 11, fracture toughness of ECC matrix slightly increases with the increase in IOTs size, which is caused by the increased tortuosity of fracture path along the interfacial transition zone (ITZ) between IOTs particles and surrounding cement paste. As the first cracking strength is proportional to the matrix fracture toughness, the increasing trend of matrix fracture toughness with the increase in IOTs size is also reflected in the corresponding increasing trend of first cracking strength (Table 4). According to the micromechanics based design theory of ECC, there are two necessary conditions that must be satisfied for achieving strain-hardening [22,23]. The first condition requires that the cracking strength  $\sigma_{cr}$  on any given crack plane be smaller than the fiber bridging capacity  $\sigma_0$ . The second condition requires that the crack tip toughness  $J_{tip}$  be less than the complementary energy  $J'_b$  of fiber bridging. Large margins between  $\sigma_0$  and  $\sigma_{cr}$ , and between  $J_{tip}$  and  $J'_b$  are both preferred for increasing the potential for saturated multiple cracking and high tensile ductility of ECC [24]. Higher matrix fracture toughness due to the incorporation of coarser IOTs suppresses the margins between  $\sigma_0$  and  $\sigma_{cr}$ , and between  $J_{tip}$  and  $J'_b$ , thus resulting in lower tensile strain capacity.

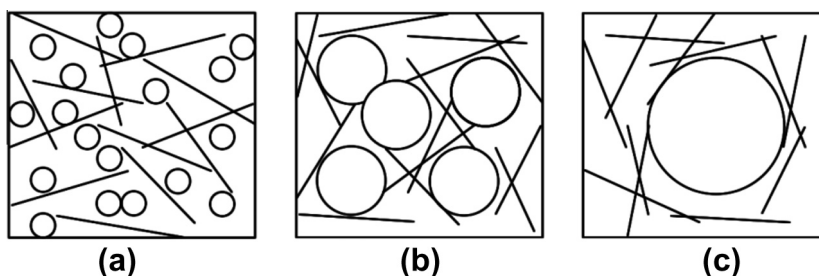
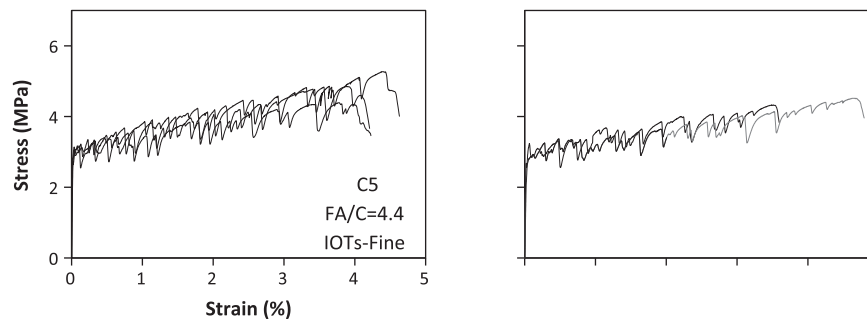


Fig. 10. Influence of aggregate size on the fiber dispersion [5] ((a) aggregate size < fiber spacing; (b) aggregate size ~ fiber spacing; and (c) aggregate size > fiber spacing).



### 3.3. Influence of aggregate type and fly ash content on the tensile properties of ECC mixtures

The uniaxial tensile stress–strain curves of ECC mixtures with different aggregate (micro-silica sand, IOTs-Fine, and IOTs-425) and different fly ash content (FA/C ratios of 2.2 and 4.4) at the age of 28 days are given in Fig. 6a and b and Fig. 12. The averaged results of three measurements of first cracking strength, tensile strength, and tensile strain capacity at 28 days are summarized in Table 6. All ECC mixtures exhibit strain hardening and ductile behavior, with tensile strain capacities ranging from 2.8% to 4.7%. The increase of fly ash content (FA/C) increases the tensile ductility of ECC mixtures, and reduces first cracking and tensile strength. This trend can be explained by the fact that increase in fly ash content tends to lower the chemical bond at fiber/matrix interface and fracture toughness of ECC matrix, while increasing the interface frictional bond [25]. The net effects of these changes in micro-scale interactions, caused by increase in fly ash content, are increases in margins between  $J_{tip}$  and  $J'_b$  and between  $\sigma_0$  and  $\sigma_{cr}$ , both of which substantially enhance the tensile ductility of ECC as discussed above.

Regardless of FA/C ratio, the tensile properties in terms of first cracking strength, tensile strength, and tensile strain capacity of ECC mixtures with IOTs-Fine and with IOTs-425 are quite similar. For each level of FA/C, ECC mixtures with micro-silica sand exhibit slightly higher tensile ductility than that with IOTs-Fine and IOTs-

425 (Table 6). This can be attributed to the fact that fracture toughness of ECC matrix with micro-silica sand is lower than that with IOTs, which is clearly reflected in the decreased first cracking strength of ECC mixtures with micro-silica sand (Table 6). The lower fracture toughness of ECC matrix with micro-silica sand is likely caused by more rounded shape and smooth surface of micro-silica sand that allows the crack at the interface between aggregate and cement paste to propagate more easily. Moreover, at a constant FA/C, the difference in tensile strength between ECC mixtures with IOTs and with micro-silica sand is fairly small. Therefore, the substitution of micro-silica sand by IOTs-Fine and IOTs-425 as aggregates in the preparation of ECC is demonstrated to have only minor negative effects on the tensile properties of ECC.

### 3.4. Influence of aggregate type and fly ash content on the compressive properties of ECC mixtures

The compressive strength test results of ECC mixtures with different aggregate and FA/C ratio at 28 days are shown in Fig. 13. The compressive strength of ECC mixtures decreases with the increase in FA/C. This is a well-documented effect caused by relatively slower secondary hydration reactions of fly ash compared to the primary hydration reactions of cement [26]. At each level of FA/C, the change in aggregate type and size leads to slight difference in compressive strengths of ECC mixtures. At FA/C of 2.2, the compressive strength of ECC mixtures ranges from 47.3 to 50.1 MPa; at

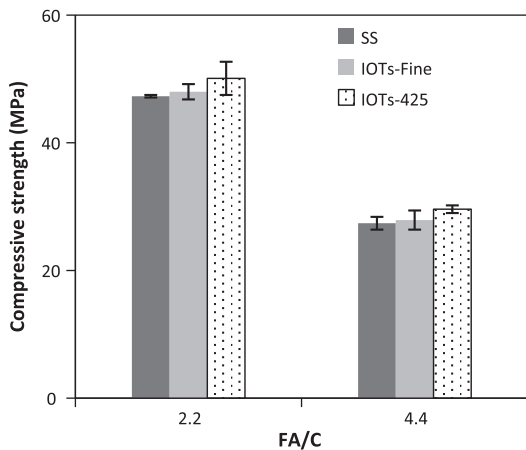


Fig. 13. Compressive strength of ECC mixtures at 28 days.

FA/C of 4.4, the compressive strength of ECC mixtures ranges from 27.4 to 29.6 MPa. This suggests that replacing micro-silica sand by IOTs with particle sizes within the size range studied herein does not have significant effect on the compressive strength of ECC mixtures.

#### 4. Conclusions

Findings from this research demonstrate the feasibility of using IOTs as aggregates in the production of green ECC. The size of IOTs was revealed to have significant influences on the fresh and hardened properties of ECC. It was found that IOTs-Fine and IOTs-425 maintain relatively good fiber dispersion and thus high tensile ductility; IOTs with particle sizes larger than IOTs-425 cause significant reduction in tensile performance. The mechanical properties in terms of tensile first cracking strength, tensile strength, tensile strain capacity, and compressive strength of ECC mixtures with IOTs-Fine or IOTs-425 are comparable to those of the standard ECC mixtures with micro-silica sand. ECC mixtures with IOTs (IOTs-Fine or IOTs-425) exhibit tensile first cracking strength of 3.0–3.9 MPa, ultimate tensile strengths of 4.7–5.8 MPa, tensile strain capacity of 2.8–4.2%, and compressive strength of 27.9–50.1 MPa at 28 days, depending on the FA/C weight ratio. The successful utilization of industrial solid waste IOTs in the preparation of ECC demonstrated in this study can potentially offer great benefits in promoting the material greenness, natural resource conservation, and environment protection.

#### Acknowledgements

Support from the National Science Foundation (CMMI 1030159) to the University of Michigan is gratefully acknowledged. Xiaoyan Huang is supported by a grant from the Chinese Scholarship Council as a visiting scholar at the University of Michigan. Wen Ni acknowledges the support from Key Laboratory of Solid Waste Treatment and Resource Recycle, Ministry of Education of China (Open research fund No.10zxgk03). The authors would also like to acknowledge Lafarge (cement), Headwaters (fly ash), WR Grace

(HRWRA), Kuraray (PVA fiber), and Shouyun (Iron ore tailings) for providing materials used in this research.

#### References

- [1] Li VC. Tailoring E.C.C. for special attributes: a review. *Int J Concr Struct Mater* 2012;6:135–44.
- [2] Li VC, Wu C, Wang S, et al. Interface tailoring for strain-hardening polyvinyl alcohol-engineered cementitious composites (PVA-ECC). *ACI Mater J* 2002;99(5):463–72.
- [3] Ahmed Shaikh Faiz Uddin, Mihashi Hirozo. A review on durability properties of strain hardening fibre reinforced cementitious composites (SHFRCC). *Cem Concr Compos* 2007;29(5):365–76.
- [4] Wang S, Li VC. Engineered cementitious composites with high-volume fly ash. *ACI Mater J* 2007;104(3):233–41.
- [5] De Koker D, Van Zijl G. Extrusion of engineered cement-based composite material. In: *Proc. BEFIB 2004*; p. 1301–10.
- [6] Li M, Li VC. Rheology, fiber dispersion, and robust properties of engineered cementitious composites. *RILEM J Mater Struct* 2012;1–16.
- [7] Yang E, Garcez E, Yang Y, et al. Development of pigmentable engineered cementitious composites for architectural elements through integrated structures and materials design. *RILEM J Mater Struct* 2012;45(3):425–32.
- [8] Wang S, Li VC. Lightweight engineered cementitious composites (ECC). In: *Proc. fourth int'l RILEM workshop on high performance fiber reinforced cement composites (HPFRCC 4)*, vol. 1; 2003. p. 379–90.
- [9] Wang S, Li VC. High early strength engineered cementitious composites. *ACI Mater J* 2006;103(2):97–105.
- [10] Kim JK, Kim JS, Ha GJ, et al. Tensile and fiber dispersion performance of ECC (engineered cementitious composites) produced with ground granulated blast furnace slag. *Cem Concr Res* 2007;37(7):1096–105.
- [11] Jian Z, Qian S, Guadalupe Sierra Beltran M, et al. Development of engineered cementitious composites with limestone powder and blast furnace slag. *RILEM J Mater Struct* 2010;43(6):803–14.
- [12] Keoleian GA, Kendall A, Dettling JE, et al. Life-cycle cost model for evaluating the sustainability of bridge decks. In: *Proc. fourth int'l workshop on life-cycle cost analysis and design of civil infrastructures systems*, Cocoa Beach, FL, USA; 2005.
- [13] Meng Y, Ni W, Zhang Y. Current state of ore tailings reusing in China. In: *Proc. high-level forum 2011 for industry development of tailings comprehensive utilization*, Beijing, China; 2011. p. 1–9 [in Chinese].
- [14] Ministry of Industry and Information Technology of the People's Republic of China (MIITPRC). Plan on the comprehensive utilization of metal ore tailings for 2010–2015. <<http://www.miit.gov.cn/n11293472/n11293832/n12843926/13158991.html>>. [in Chinese].
- [15] Huang X, Ranade R, Li VC. Feasibility study of developing green ECC using iron ore tailings (IOTs) powder as cement replacement. *ASCE J Mater Civ Eng* 2012. [http://ascelibrary.org/doi/abs/10.1061/\(ASCE\)MT.1943-5533.0000674](http://ascelibrary.org/doi/abs/10.1061/(ASCE)MT.1943-5533.0000674).
- [16] Ranade R, Stults MD, Li VC, et al. Development of high strength high ductility concrete. In: *Proc second int'l RILEM conference on strain hardening cementitious composites (SHCC2)*, Rio de Janeiro, Brazil; 2011. p. 1–8.
- [17] Li VC, Mishra DK, Wu HC. Matrix design for pseudo strain-hardening fiber reinforced cementitious composites. *RILEM J Mater Struct* 1995;28(183):586–95.
- [18] JSCE. Recommendations for design and construction of high performance fiber reinforced cement composites with multiple fine cracks. Tokyo: Japan Soc. of Civil Engineers; 2008.
- [19] Lee BY, Kim JK, Kim JS, et al. Quantitative evaluation technique of polyvinyl alcohol (PVA) fiber dispersion in engineered cementitious composites. *Cem Concr Compos* 2009;31(6):408–17.
- [20] Yang E, Wang S, Yang Y, et al. Fiber-bridging constitutive law of engineered cementitious composites. *J Adv Concr Technol* 2008;6(1):181–93.
- [21] Li VC, Leung CKY. Steady state and multiple cracking of short random fiber composites. *ASCE J Eng Mech* 1992;118(11):2246–64.
- [22] Li VC. Engineered cementitious composites-tailored composites through micromechanical modeling. In: Banthia N, Bentur A, Mufti A, editors. *Fiber reinforced concrete: present and the future*. Montreal, QC, Canada: Canadian Society for Civil Engineering; 1997. p. 64–97.
- [23] Kanda T, Li VC. Practical design criteria for saturated pseudo strain hardening behavior in ECC. *J Adv Concr Technol* 2006;4(1):59–72.
- [24] Yang E, Yang Y, Li VC. Use of high volumes of fly ash to improve ECC mechanical properties and material greenness. *ACI Mater J* 2007;104(6):620–8.
- [25] Mehta P, Monteiro PJM. *Concrete properties and materials*. 3rd ed. McGraw Hill; 2005.